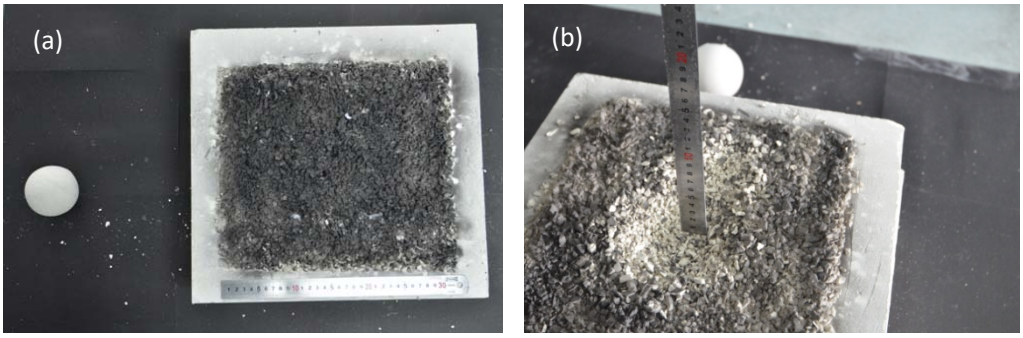

Fig. 7 Photographs of a cushion (a) before and (b) after a rock impact experiment

Table 1 The COR of block collisions with the plate

H=1.2m ,h=0cm,d=0mm						Average Value
r=2cm		0.363	0.368	0.421		0.384
r=3cm		0.398	0.428	0.437		0.421
r=4cm		0.386	0.482	0.443		0.437
r=5cm		0.403	0.458	0.471		0.444

Table 2 Comparison of the COR of different blocks released from a height of 1.2m

H=1.2m,r=2cm,h=2cm						Average Value
d=2mm		0.310	0.329	0.339		0.326
d=6mm		0.298	0.348	0.35		0.332
d=10mm		0.319	0.343	0.376		0.346
d=14mm		0.314	0.344	0.371		0.343
d=18mm	0.262	0.291	0.337	0.416	0.443	0.348
d=24mm	0.234	0.288	0.371	0.403	0.421	0.354

H=1.2m,r=2cm,h=4cm						Average Value
d=2mm		0.281	0.285	0.316		0.294
d=6mm		0.292	0.338	0.345		0.325
d=10mm		0.261	0.314	0.331		0.302
d=14mm		0.285	0.324	0.360		0.323
d=18mm	0.215	0.252	0.323	0.376	0.386	0.317
d=24mm	0.267	0.270	0.304	0.362	0.403	0.312

H=1.2m,r=2cm,h=6cm						Average Value
d=2mm		0.240	0.267	0.270		0.259
d=6mm		0.239	0.277	0.306		0.274
d=10mm		0.246	0.283	0.317		0.282
d=14mm		0.251	0.267	0.331		0.283
d=18mm	0.231	0.259	0.299	0.345	0.382	0.301
d=24mm	0.226	0.261	0.291	0.336	0.370	0.296

H=1.2m,r=2cm,h=8cm						Average Value
d=2mm		0.215	0.243	0.271		0.243

d=6mm		0.211	0.261	0.290		0.254
d=10mm		0.216	0.261	0.312		0.263
d=14mm		0.223	0.286	0.304		0.271
d=18mm	0.205	0.225	0.285	0.321	0.356	0.277
d=24mm	0.193	0.206	0.292	0.354	0.371	0.284

9

H=1.2m,r=2cm,h=10cm						Average Value
d=2mm		0.201	0.245	0.277		0.241
d=6mm		0.198	0.250	0.293		0.247
d=10mm		0.226	0.251	0.288		0.255
d=14mm		0.210	0.253	0.311		0.258
d=18mm	0.190	0.192	0.273	0.327	0.363	0.264
d=24mm	0.204	0.214	0.292	0.325	0.350	0.277

10

H=1.2m,r=2cm,h=12cm						Average Value
d=2mm		0.207	0.218	0.259		0.228
d=6mm		0.190	0.236	0.273		0.233
d=10mm		0.214	0.225	0.302		0.247
d=14mm		0.200	0.243	0.313		0.252
d=18mm	0.189	0.198	0.236	0.319	0.328	0.251
d=24mm	0.198	0.221	0.251	0.326	0.343	0.266

11

H=1.2m,r=2cm,h=14cm						Average Value
d=2mm		0.184	0.230	0.246		0.22
d=6mm		0.199	0.214	0.283		0.232
d=10mm		0.204	0.251	0.265		0.24
d=14mm		0.183	0.224	0.301		0.236
d=18mm	0.162	0.196	0.260	0.291	0.314	0.249
d=24mm	0.194	0.208	0.250	0.316	0.353	0.258

12

13

14

H=1.2m,r=3cm,h=2cm						Average Value
d=2mm		0.313	0.338	0.351		0.334
d=6mm		0.326	0.348	0.349		0.341
d=10mm		0.308	0.354	0.379		0.347
d=14mm		0.311	0.342	0.409		0.354
d=18mm	0.261	0.333	0.336	0.387	0.396	0.352
d=24mm	0.256	0.322	0.369	0.413	0.420	0.368

15

H=1.2m,r=3cm,h=4cm						Average Value
d=2mm		0.261	0.316	0.329		0.302
d=6mm		0.276	0.309	0.360		0.315

d=10mm		0.267	0.329	0.352		0.316
d=14mm		0.282	0.320	0.379		0.327
d=18mm	0.245	0.298	0.314	0.366	0.381	0.326
d=24mm	0.253	0.276	0.321	0.405	0.415	0.334

16

H=1.2m,r=3cm,h=6cm						Average Value
d=2mm		0.254	0.273	0.304		0.277
d=6mm		0.262	0.281	0.309		0.284
d=10mm		0.255	0.288	0.321		0.288
d=14mm		0.283	0.311	0.360		0.318
d=18mm	0.185	0.261	0.300	0.366	0.384	0.309
d=24mm	0.248	0.248	0.337	0.390	0.393	0.325

17

H=1.2m,r=3cm,h=8cm						Average Value
d=2mm		0.229	0.235	0.277		0.247
d=6mm		0.213	0.270	0.303		0.262
d=10mm		0.241	0.247	0.313		0.267
d=14mm		0.223	0.264	0.332		0.273
d=18mm	0.214	0.220	0.303	0.320	0.341	0.281
d=24mm	0.235	0.261	0.292	0.323	0.354	0.292

18

H=1.2m,r=3cm,h=10cm						Average Value
d=2mm		0.212	0.233	0.266		0.237
d=6mm		0.223	0.240	0.275		0.246
d=10mm		0.228	0.246	0.288		0.254
d=14mm		0.213	0.271	0.302		0.262
d=18mm	0.192	0.211	0.251	0.309	0.324	0.257
d=24mm	0.211	0.232	0.246	0.326	0.341	0.268

19

H=1.2m,r=3cm,h=12cm						Average Value
d=2mm		0.194	0.220	0.264		0.226
d=6mm		0.199	0.231	0.287		0.239
d=10mm		0.228	0.234	0.264		0.242
d=14mm		0.204	0.256	0.284		0.248
d=18mm	0.213	0.228	0.242	0.295	0.320	0.255
d=24mm	0.186	0.217	0.259	0.301	0.336	0.259

20

H=1.2m,r=3cm,h=14cm						Average Value
d=2mm		0.172	0.206	0.276		0.218
d=6mm		0.203	0.215	0.254		0.224
d=10mm		0.188	0.224	0.275		0.229
d=14mm		0.178	0.229	0.286		0.231
d=18mm	0.186	0.192	0.244	0.302	0.335	0.246

d=24mm	0.191	0.228	0.246	0.312	0.343	0.262

21

22

23

H=1.2m,r=4cm,h=2cm						Average Value
d=2mm		0.316	0.338	0.354		0.336
d=6mm		0.329	0.343	0.372		0.348
d=10mm		0.333	0.351	0.384		0.356
d=14mm		0.321	0.358	0.416		0.365
d=18mm	0.285	0.329	0.371	0.401	0.411	0.367
d=24mm	0.313	0.334	0.369	0.413	0.432	0.372

24

H=1.2m,r=4cm,h=4cm						Average Value
d=2mm		0.284	0.307	0.336		0.309
d=6mm		0.298	0.319	0.346		0.321
d=10mm		0.288	0.310	0.347		0.315
d=14mm		0.308	0.316	0.351		0.325
d=18mm	0.263	0.295	0.339	0.368	0.374	0.334
d=24mm	0.275	0.309	0.326	0.394	0.410	0.343

25

H=1.2m,r=4cm,h=6cm						Average Value
d=2mm		0.267	0.279	0.294		0.28
d=6mm		0.294	0.304	0.329		0.309
d=10mm		0.273	0.286	0.317		0.292
d=14mm		0.280	0.292	0.304		0.292
d=18mm	0.257	0.282	0.303	0.351	0.384	0.312
d=24mm	0.240	0.294	0.322	0.359	0.367	0.325

26

H=1.2m,r=4cm,h=8cm						Average Value
d=2mm		0.249	0.250	0.269		0.256
d=6mm		0.250	0.267	0.296		0.271
d=10mm		0.248	0.274	0.306		0.276
d=14mm		0.252	0.271	0.299		0.274
d=18mm	0.235	0.263	0.291	0.325	0.344	0.293
d=24mm	0.259	0.267	0.298	0.341	0.367	0.302

27

H=1.2m,r=4cm,h=10cm						Average Value
d=2mm		0.239	0.249	0.268		0.252
d=6mm		0.235	0.261	0.278		0.258
d=10mm		0.247	0.264	0.296		0.269
d=14mm		0.254	0.249	0.292		0.265
d=18mm	0.226	0.243	0.276	0.324	0.331	0.281
d=24mm	0.231	0.236	0.277	0.321	0.354	0.278

28

H=1.2m,r=4cm,h=12cm						Average Value
d=2mm		0.229	0.231	0.248		0.236
d=6mm		0.221	0.244	0.270		0.245
d=10mm		0.216	0.227	0.268		0.237
d=14mm		0.207	0.239	0.283		0.243
d=18mm	0.186	0.208	0.251	0.297	0.319	0.252
d=24mm	0.217	0.218	0.272	0.284	0.326	0.258

29

H=1.2m,r=4cm,h=14cm						Average Value
d=2mm		0.217	0.218	0.237		0.224
d=6mm		0.215	0.231	0.259		0.235
d=10mm		0.196	0.229	0.271		0.232
d=14mm		0.219	0.224	0.268		0.237
d=18mm	0.181	0.207	0.256	0.281	0.314	0.248
d=24mm	0.196	0.219	0.247	0.293	0.335	0.253

30

31

32

H=1.2m,r=5cm,h=2cm						Average Value
d=2mm		0.328	0.336	0.356		0.34
d=6mm		0.320	0.342	0.364		0.342
d=10mm		0.324	0.351	0.393		0.356
d=14mm		0.342	0.364	0.398		0.368
d=18mm	0.317	0.338	0.374	0.401	0.426	0.371
d=24mm	0.302	0.354	0.365	0.421	0.437	0.38

33

H=1.2m,r=5cm,h=4cm						Average Value
d=2mm		0.316	0.317	0.339		0.324
d=6mm		0.297	0.306	0.330		0.311
d=10mm		0.294	0.321	0.354		0.323
d=14mm		0.318	0.340	0.374		0.344
d=18mm	0.318	0.321	0.322	0.386	0.397	0.343
d=24mm	0.284	0.328	0.355	0.373	0.403	0.352

34

H=1.2m,r=5cm,h=6cm						Average Value
d=2mm		0.286	0.286	0.301		0.291
d=6mm		0.274	0.287	0.315		0.292
d=10mm		0.301	0.324	0.329		0.318
d=14mm		0.291	0.298	0.338		0.309
d=18mm	0.244	0.286	0.314	0.378	0.398	0.326
d=24mm	0.270	0.293	0.316	0.381	0.401	0.33

35

H=1.2m,r=5cm,h=8cm						Average Value
d=2mm		0.254	0.262	0.279		0.265
d=6mm		0.270	0.276	0.294		0.28
d=10mm		0.261	0.294	0.309		0.288
d=14mm		0.272	0.283	0.324		0.293
d=18mm	0.226	0.256	0.294	0.356	0.362	0.302
d=24mm	0.234	0.286	0.291	0.362	0.374	0.313

H=1.2m,r=5cm,h=10cm						Average Value
d=2mm		0.247	0.261	0.281		0.263
d=6mm		0.233	0.273	0.289		0.265
d=10mm		0.249	0.257	0.301		0.269
d=14mm		0.250	0.268	0.298		0.272
d=18mm	0.208	0.237	0.261	0.315	0.320	0.271
d=24mm	0.221	0.255	0.273	0.336	0.373	0.288

H=1.2m,r=5cm,h=12cm						Average Value
d=2mm		0.230	0.236	0.254		0.24
d=6mm		0.213	0.251	0.265		0.243
d=10mm		0.220	0.245	0.291		0.252
d=14mm		0.242	0.240	0.289		0.257
d=18mm	0.197	0.224	0.242	0.311	0.342	0.259
d=24mm	0.208	0.209	0.261	0.328	0.337	0.266

H=1.2m,r=5cm,h=14cm						Average Value
d=2mm		0.207	0.217	0.236		0.22
d=6mm		0.204	0.229	0.257		0.23
d=10mm		0.227	0.234	0.250		0.237
d=14mm		0.215	0.241	0.270		0.242
d=18mm	0.184	0.189	0.235	0.278	0.304	0.234
d=24mm	0.201	0.218	0.258	0.286	0.316	0.254

Table 3 Comparison of the COR for different blocks colliding with an 8-cm thick cushion

h=8cm,r=2cm,H=0.4m						Average Value
d=2mm		0.197	0.214	0.237		0.216
d=6mm		0.221	0.222	0.241		0.228
d=10mm		0.216	0.228	0.264		0.236
d=14mm		0.223	0.256	0.283		0.254
d=18mm	0.204	0.201	0.261	0.306	0.311	0.256
d=24mm	0.203	0.221	0.264	0.295	0.316	0.260

h=8cm,r=2cm,H=0.8m						Average Value
d=2mm		0.219	0.231	0.237		0.229
d=6mm		0.200	0.248	0.254		0.234
d=10mm		0.220	0.242	0.273		0.245
d=14mm		0.213	0.246	0.270		0.243
d=18mm	0.214	0.221	0.274	0.291	0.327	0.262
d=24mm	0.191	0.212	0.271	0.318	0.331	0.267

h=8cm,r=2cm,H=1.2m						Average Value
d=2mm		0.228	0.236	0.265		0.243
d=6mm		0.217	0.267	0.278		0.254
d=10mm		0.231	0.262	0.296		0.263
d=14mm		0.222	0.283	0.308		0.271
d=18mm	0.207	0.226	0.287	0.318	0.336	0.277
d=24mm	0.226	0.247	0.299	0.306	0.337	0.284

h=8cm,r=2cm,H=1.6m						Average Value
d=2mm		0.232	0.239	0.258		0.243
d=6mm		0.240	0.243	0.273		0.252
d=10mm		0.223	0.294	0.296		0.271
d=14mm		0.245	0.287	0.338		0.290
d=18mm	0.221	0.249	0.279	0.321	0.332	0.283
d=24mm	0.218	0.234	0.276	0.336	0.359	0.282

h=8cm,r=3cm,H=0.4m						Average Value
d=2mm		0.208	0.227	0.237		0.224
d=6mm		0.212	0.226	0.255		0.231
d=10mm		0.228	0.231	0.270		0.243
d=14mm		0.216	0.251	0.289		0.252
d=18mm	0.186	0.222	0.267	0.306	0.316	0.265
d=24mm	0.179	0.211	0.272	0.321	0.331	0.268

h=8cm,r=3cm,H=0.8m						Average Value
d=2mm		0.222	0.235	0.251		0.236
d=6mm		0.218	0.247	0.264		0.243
d=10mm		0.235	0.251	0.306		0.264
d=14mm		0.220	0.274	0.292		0.262
d=18mm	0.231	0.242	0.254	0.305	0.329	0.267

d=24mm	0.224	0.234	0.270	0.324	0.354	0.276

53

h=8cm,r=3cm,H=1.2m						Average Value
d=2mm		0.229	0.243	0.269		0.247
d=6mm		0.241	0.265	0.28		0.262
d=10mm		0.234	0.27	0.297		0.267
d=14mm		0.221	0.288	0.310		0.273
d=18mm	0.198	0.239	0.283	0.321	0.334	0.281
d=24mm	0.227	0.251	0.287	0.338	0.356	0.292

54

h=8cm,r=3cm,H=1.6m						Average Value
d=2mm		0.242	0.251	0.269		0.254
d=6mm		0.228	0.279	0.288		0.265
d=10mm		0.261	0.284	0.313		0.286
d=14mm		0.256	0.286	0.325		0.289
d=18mm	0.262	0.276	0.291	0.312	0.323	0.293
d=24mm	0.214	0.272	0.295	0.336	0.351	0.301

55

56

57

h=8cm,r=4cm,H=0.4m						Average Value
d=2mm		0.220	0.227	0.246		0.231
d=6mm		0.233	0.234	0.259		0.242
d=10mm		0.212	0.241	0.264		0.239
d=14mm		0.241	0.252	0.299		0.264
d=18mm	0.209	0.239	0.253	0.294	0.321	0.262
d=24mm	0.213	0.236	0.278	0.314	0.316	0.276

58

h=8cm,r=4cm,H=0.8m						Average Value
d=2mm		0.223	0.247	0.265		0.245
d=6mm		0.248	0.252	0.271		0.257
d=10mm		0.236	0.257	0.293		0.262
d=14mm		0.260	0.285	0.316		0.287
d=18mm	0.216	0.247	0.287	0.324	0.338	0.286
d=24mm	0.224	0.230	0.302	0.338	0.351	0.290

59

h=8cm,r=4cm,H=1.2m						Average Value
d=2mm		0.245	0.254	0.269		0.256
d=6mm		0.230	0.287	0.296		0.271
d=10mm		0.249	0.281	0.298		0.276
d=14mm		0.268	0.278	0.306		0.284
d=18mm	0.225	0.256	0.291	0.332	0.348	0.293
d=24mm	0.248	0.282	0.303	0.321	0.367	0.302

60

h=8cm,r=4cm,H=1.6m						Average Value
d=2mm		0.243	0.257	0.283		0.261
d=6mm		0.269	0.282	0.304		0.285
d=10mm		0.254	0.283	0.321		0.286
d=14mm		0.237	0.327	0.333		0.299
d=18mm	0.234	0.273	0.306	0.354	0.375	0.311
d=24mm	0.211	0.262	0.307	0.361	0.394	0.310

61

62

63

64

65

h=8cm,r=5cm,H=0.4m						Average Value
d=2mm		0.229	0.231	0.248		0.236
d=6mm		0.243	0.247	0.269		0.253
d=10mm		0.211	0.256	0.283		0.25
d=14mm		0.232	0.259	0.298		0.263
d=18mm	0.213	0.228	0.284	0.316	0.354	0.276
d=24mm	0.207	0.250	0.281	0.321	0.348	0.284

66

h=8cm,r=5cm,H=0.8m						Average Value
d=2mm		0.239	0.246	0.271		0.252
d=6mm		0.252	0.268	0.281		0.267
d=10mm		0.261	0.284	0.304		0.283
d=14mm		0.230	0.288	0.298		0.272
d=18mm	0.218	0.253	0.291	0.338	0.351	0.294
d=24mm	0.206	0.247	0.316	0.331	0.383	0.298

67

h=8cm,r=5cm,H=1.2m						Average Value
d=2mm		0.258	0.259	0.278		0.265
d=6mm		0.237	0.300	0.303		0.28
d=10mm		0.259	0.286	0.319		0.288
d=14mm		0.247	0.287	0.345		0.293
d=18mm	0.251	0.266	0.298	0.342	0.354	0.302
d=24mm	0.236	0.272	0.306	0.361	0.381	0.313

68

h=8cm,r=5cm,H=1.6m						Average Value
d=2mm		0.244	0.279	0.296		0.273
d=6mm		0.268	0.284	0.309		0.287
d=10mm		0.254	0.307	0.336		0.299
d=14mm		0.271	0.311	0.348		0.31
d=18mm	0.246	0.258	0.307	0.359	0.387	0.308

d=24mm	0.225	0.279	0.338	0.349	0.368	0.322

Table 4. Orthogonal test results

r=2cm,H=0.4m,h=2cm,d=2mm			Average Value
0.269	0.274	0.291	0.278
r=2cm,H=0.8m,h=4cm,d=6mm			Average Value
0.253	0.268	0.298	0.273
r=2cm,H=1.2m,h=6cm,d=10mm			Average Value
0.255	0.278	0.313	0.282
r=2cm,H=1.6m,h=8cm,d=14mm			Average Value
0.266	0.298	0.321	0.295

r=3cm,H=0.4m,h=2cm,d=6mm			Average Value
0.287	0.287	0.308	0.294
r=3cm,H=0.8m,h=4cm,d=2mm			Average Value
0.252	0.261	0.282	0.265
r=3cm,H=1.2m,h=6cm,d=14mm			Average Value
0.275	0.319	0.357	0.317
r=3cm,H=1.6m,h=8cm,d=10mm			Average Value
0.264	0.273	0.303	0.280

r=4cm,H=0.4m,h=4cm,d=10mm			Average Value
0.265	0.304	0.319	0.296
r=4cm,H=0.8m,h=2cm,d=14mm			Average Value
0.304	0.354	0.356	0.338
r=4cm,H=1.2m,h=8cm,d=2mm			Average Value
0.232	0.261	0.275	0.256
r=4cm,H=1.6m,h=6cm,d=6mm			Average Value
0.247	0.286	0.319	0.284

r=5cm,H=0.4m,h=4cm,d=14mm			Average Value
0.283	0.300	0.344	0.309
r=5cm,H=0.8m,h=2cm,d=10mm			Average Value
0.288	0.336	0.360	0.328
r=5cm,H=1.2m,h=8cm,d=6mm			Average Value
0.251	0.291	0.298	0.280
r=5cm,H=1.6m,h=6cm,d=2mm			Average Value
0.249	0.277	0.293	0.273

r=2cm,H=0.4m,h=8cm,d=2mm			Average Value
0.199	0.218	0.231	0.216
r=2cm,H=0.8m,h=6cm,d=6mm			Average Value

0.239	0.267	0.289	0.265
r=2cm,H=1.2m,h=4cm,d=10mm			Average Value
0.273	0.298	0.335	0.302
r=2cm,H=1.6m,h=2cm,d=14mm			Average Value
0.319	0.361	0.394	0.358

r=3cm,H=0.4m,h=8cm,d=6mm			Average Value
0.211	0.239	0.243	0.231
r=3cm,H=0.8m,h=6cm,d=2mm			Average Value
0.243	0.258	0.267	0.256
r=3cm,H=1.2m,h=4cm,d=14mm			Average Value
0.291	0.344	0.346	0.327
r=3cm,H=1.6m,h=2cm,d=10mm			Average Value
0.324	0.347	0.382	0.351

r=4cm,H=0.4m,h=6cm,d=10mm			Average Value
0.254	0.284	0.323	0.287
r=4cm,H=0.8m,h=8cm,d=14mm			Average Value
0.259	0.273	0.311	0.281
r=4cm,H=1.2m,h=2cm,d=2mm			Average Value
0.315	0.337	0.356	0.336
r=4cm,H=1.6m,h=4cm,d=6mm			Average Value
0.291	0.312	0.351	0.318

r=5cm,H=0.4m,h=6cm,d=14mm			Average Value
0.272	0.295	0.309	0.292
r=5cm,H=0.8m,h=8cm,d=10mm			Average Value
0.193	0.284	0.348	0.275
r=5cm,H=1.2m,h=2cm,d=6mm			Average Value
0.323	0.346	0.372	0.347
r=5cm,H=1.6m,h=4cm,d=2mm			Average Value
0.270	0.289	0.323	0.294

MogoEdit

CERTIFICATE OF ENGLISH EDITING

This is to certify that the manuscript entitled

The effects of gravel cushion particle size and thickness on coefficient of restitution under the rockfall impacts

commissioned to us has been carefully edited by a native English-speaking editor of MogoEdit, and the grammar, spelling, and punctuation have been verified and corrected where needed. Based on this review, we believe that the language in this paper meets academic journal requirements. Please contact us with any questions.

MOGOEDIT MOGO INTERNET TECHNOLOGY CO., LTD.

Gang Zhang

Dr. Gang Zhang
Founder & CEO of MogoEdit

Date of Issue
March 15, 2018

Disclaimer: The changes in the document may be accepted or rejected by the authors in their sole discretion after our editing. However, MogoEdit is not responsible for revisions made to the document after our edit on **March 15, 2018.**

MogoEdit is a professional English editing company who provides English language editing, translation, and publication support services to individuals and corporate customers worldwide. As a company invested by the affiliate fund of Chinese Academy of Science, MogoEdit is one of the leading language editing service providers in China, whose clients come from more than 1000 universities and research institutes.
MogoEdit Website: http://en.mogoedit.com/
500+ native English editors: http://en.mogoedit.com/editors

Mogo make the world flatter

Mogo Internet Technology Co., LTD.
No. 25, 1st Gaoxin Road, Xi'an 710075, PR China +86 02988317483 support@mogoedit.com

The effects of gravel cushion particle size and thickness on coefficient of restitution under the rockfall impacts

Zhu Chun[1,2,3],Wang Dongsheng[2,3],Xia Xing[2,3],Tao ZhiGang[2,3], HeManChao[1,2,3], Cao Chen[1]*

Corresponding Email：zhuchuncumtb@163.com;

ccao@jlu.edu.cn (Corresponding Author)

(1. College of Construction Engineering, Jilin University, Changchun 130026, China)

(2. State Key Laboratory for Geomechanics & Deep Underground Engineering, Beijing 100083, China)

(3. School of Mechanics and Civil Engineering, China University of Mining & Technology, Beijing 100083,China)

Abstracts: Gravel cushions are widely used for energy-absorption in open-pit mine rockfall protection. This study investigates the energy consumption and buffering mechanism of different thicknesses and particle sizes of gravel cushion under the effects of impact. A series of laboratory tests were conducted for different cushion parameters, varying both the radius (and hence mass) of the falling block and its drop height. Tests using a constant rockfall release height indicate that changes in cushion thickness have an appreciably different effect on the coefficient of restitution (COR) of the cushion under different impact energies. Tests with identical cushion thickness, but with blocks of different radii colliding with the cushion show that the range in COR for blocks of a large radius is greater than for blocks with a relatively small radius. The degree of influence of the particle size and thickness of the cushion on the COR when rockfall moves through the cushion was also studied .Based on the orthogonal test principle, 32 orthogonal tests are conducted to explore the degree of influence of each factor on the damage depth,*L,* of the cushion and the COR of the collision between rockfall and cushion. The results show that cushion thickness,*h*, should be a primary consideration during cushion design, as an appropriate cushion not only effectively reduces COR but also remains more stable. This study thus provides a widely-applicable theoretical and practical basis for the design of cushions for mitigating rockfall hazard in open pit mines.

Keywords: Rockfall; cushion thickness; laboratory test; particle size; coefficient of restitution (COR).

1 Introduction

Rockfall constitutes a serious hazard in the working areas and facilities of the world's open-pit mines. Where slope surfaces are seriously weathered and the disturbing forces from mining are strong, landslides and rock-body collapse are prone to occur during rainfall. In rockfall, rocks roll down slope due to instability caused by gravity or exogenic action and come to rest at an obstacle or in the gentler part of the slope (Huang et al., 2007). Rockfall is widely distributed and occurs suddenly, posing a serious threat to life and property (Pantelidis, 2009; Pantelidis, 2010). In response to frequent rockfall disasters in recent years, numerous scholars in China and abroad have conducted in-depth studies into the characteristics of rockfall movement through theoretical analysis, field tests, and numerical simulation. For example, the collision rebound phenomenon of test blocks on a sandy slope has been studied through indoor small-scale, mid-sized and large-scale tests (Heidenreich, 2004; Labiouse, 2009).The effectiveness of protection measures and their influence on rockfall hazard zoning have also been evaluated. For example, Howaldetal.(2017) evaluated the protective capacity of existing and newly proposed protection measures and considered the possible reclassification of hazard as a function of the mitigation role played by the measure. Mignelli et al.(2014), meanwhile, applied a rockfall risk management approach to the road infrastructure network of the Regione Autonoma Valle D'Aosta in order to

calculate the level of risk and the potential for its reduction by rockfall protection devices. A comparative analysis of road accidents in the Aosta Valley was then undertaken to verify the methodology. Thornton et al. (1998) used Hertz contact theory, the view that material accords with ideal elastic-plastic characteristics, to study the modes of calculation of the normal and tangential collision coefficients of restitution of spheres. The effect of shape has been examined by performing tests with spherical and cubic blocks, finding that spherical blocks show higher and more consistent COR values than cubic blocks (Asteriou et al., 2016).Numerical simulation software has been adopted to analyze the characteristics of rockfall movement. The software RocFall 3.0 has been adopted indam construction, road construction andthe protection ofhistorical placesto calculate the velocity and locus of rockfalland avoid damage to theproject(Topal et al., 2006; Koleini and Van Rooy, 2011; Saroglou et al., 2012; Sadagah, 2015).State-of-the-art simulation techniques incorporating nonsmooth contact dynamics and multibody dynamics have been applied to and adapted for the efficient simulation of rockfall trajectories, and the influence of rock geometry on rockfall dynamics has been studied through numerical simulation (Leineet al., 2014).

The research outlined above indicates that several types of protection measure can be effective in controlling rockfall. Trees have a significant blocking effect on rolling rocks. Interception influence tests on the effect of trees on rockfall have been designed based on analysis of the velocity change, the distance traveled by the rockfall, and the probability of collision between trees and rockfall (Huang, 2010;Notaro, 2012; Monnetet al., 2017). Semi-rigid rockfall protection barriers have been installed along areas threatened by rockfall events, and numerical investigation of semi-rigid rockfall protection barriers has been carried out to obtain essential structural information such as the energy-absorption capacity of such barriers (Miranda et al., 2015).A large-scale field test of the impact caused by rockfallon reinforced concrete beams has been conductedandthe process of dynamic response studied and compared with the results of numerical simulation (Kishi et al., 2002; Bhatti et al., 2009; Kishi et al., 2010; Bhatti et al. 2010).Concrete barriers are classified as rigid barriers, as they absorb most of the impact and all of the residual kinetic energy of the falling rock instead of dissipating it as do flexible nets. Experience has shown that rigid walls have a tendency to break under high-impact loads and may shatter, sometimes violently (Badger et al., 2009). A method whereby short concrete-filled steel tubes were inserted between the pillars and cover plate of a rock shed was proposed, and the deformation and energy absorption characteristics of the supporting member were studied through tests and theoretical analysis (Delhomme et al., 2005; Mommessin et al., 2004). Kawahara et al.(2006) conducted a large number of experiments for different soils under different combinations of falling mass and drop height and studied the influence of soil characteristics on the impact response to rockfall. Furthermore, Lambert et al. (2014) conducted real-scale impact experiments with impact energies ranging from 200 to 2200 kJ. They studied the response of rockfall protection embankments composed of a 4-m high cellular wall when exposed to a rock impact and compared this with previous real-scale experiments on other types of embankment. Finally, Sun et al. (2016) used a tire cushion layer to absorb rockfall impact, utilizing the radial deformation of the tire. They built a reinforced concrete structure model with a tire cushion layer and carried out artificial rockfall tests.

The protection research outlined above is mainly applicable to conventional human settlements, and it is expensive and inconvenient to use these measures to control rockfall in an

open-pit mine. A relatively common way of preventing and controlling rockfall hazard in an open-pit mine is to lay an energy-consuming layeron a safety platform (Heierli et al., 1981; Labiouse et al., 1996). However, research into such cushions seldom considers the effects of the particle size of the cushion on the characteristics of rockfall movement. In particular, the combined effects of the particle size and thickness of a gravel cushion on the coefficient of restitution (COR) have not yet been explored. A large amount of mullock is produced during mining, and this can be broken into particles of different sizes in a crusher and used to pave the platform as an energy-consuming layer. A certain thickness of gravel cushion on the platform can act as a buffer, effectively absorbing the impact energy of rockfall and reducing the impact load on the protective structure while also reducing the kinetic energy of the rockfall and causing it to stall. Because the impact between the rockfall and gravel cushion is of short duration, it involves complicated elastic-plastic deformation and energy conversion, and the energy absorption performance of gravel cushions of different thicknesses and particle sizes are quite different under rockfall impacts. Determining the energy-consumption buffering mechanism of a gravel cushion and calculating the subsequent rockfall movement has become the key to cushion design. Therefore, to control rockfalls effectively, it is necessary to further study the effects of the particle size and thickness of the cushion on COR under rockfall impacts.

2Coefficient of restitution

It is challenging to predict the trajectory of rebound for a rockfall because it is influenced by several parameters such as the strength, roughness, stiffness, and inclination of the slope and blocks (Labiouse and Heidenreich, 2009). However, the coefficient of restitution (COR) is widely used for this purpose (Giani, 1992).

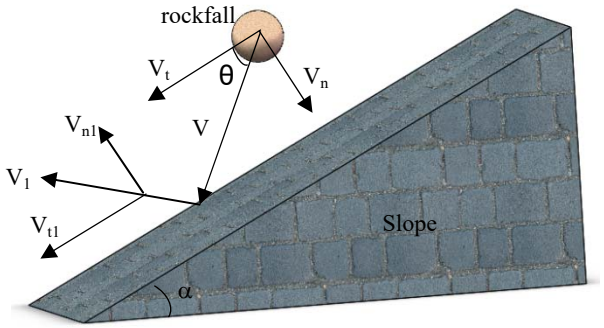

Fig.1 Motion model of rockfall

The definitions of COR are various (Chau et al., 2002) but for a block impacting a rocky slope (Figure 1), it can be defined on the basis of the theory of inelastic collision as:

$$V_{COR} = \left|\frac{V_1}{V}\right|, \quad (1)$$

where V and V_1 are the magnitudes of the incident and rebound velocities at the locus, respectively (m/s).

V_{COR} has normal and tangential components, and the normal (R_n) and tangential (R_t) coefficients are defined as:

$$R_n = \left|\frac{V_{n1}}{V_n}\right| \text{ and } R_t = \left|\frac{V_{t1}}{V_t}\right|, \quad (2)$$

Where R_n and R_t are the normal and tangential restitution coefficients, respectively, and V_n and V_{n1} are the normal components and V_t and V_{t1} are the tangential components of the velocity of the block, before and after the impact, respectively (m/s).

The total energy, E, of the block consists of the translational (E_0) and rotational (E_W) energy:

$$\mathrm{E} = E_0 + E_w = \frac{1}{2}mv^2 + \frac{1}{2}I\omega^2, \quad (3)$$

and the total energy coefficient ($\mathrm{ET_{COR}}$) is proposed to be:

$$\mathrm{ET_{COR}} = \frac{\frac{1}{2}mV_1{}^2 + \frac{1}{2}I\omega_1{}^2}{\frac{1}{2}mV^2 + \frac{1}{2}I\omega^2} = \frac{0.6mV_1{}^2}{0.6mV^2} = \frac{V_1{}^2}{V^2} = \mathrm{V_{COR}}{}^2, \quad (4)$$

Where m is the mass of the block, I is its moment of inertia, and ω and ω_1 are the angular velocity before and after the impact, respectively.

When a dangerous rock-body breaks away from the parent body, it will inevitably generate collisions with the slope during the rolling process and lose energy. A formula for the approximate calculation of the total kinetic energy of the rockfall has been derived from engineering surveys (Yang et al., 2005; Zhu et al. 2018):

$$\mathrm{E} = E_0 + E_w = 1.2E_0 = 0.6mV^2 = 0.6m(V_n{}^2 + V_t{}^2), \quad (5)$$

3 Experimental Studies

3.1 Experimental material and apparatus

In order to study the effects of the particle size and thickness of the cushion on COR under rockfall impacts conveniently, a high-strength gypsum material was adopted to simulate the rockfall. A previous study (Chau et al., 2002) recommends a moisture content of 30–50% for the sample, so in this study all samples were given a moisture content of 40%. These consisted of spherical blocks with diameters of 2cm, 3cm, 4cm and 5cm (Figure 2)and six standard 5cm-diameter by10cm-highcylindrical samples for determining the uniaxial compressive strength of the gypsum materials. The uniaxial compression test is shown in Figure 3. Due to the inherent error associated with the test, the ultimate compressive strength of the six samples is different, so the average value is taken as the compressive strength of the material. The average value at which the specimens are destroyed is 6.48Mpa, indicating that a gypsum sample with 40% moisture content is strong enough to prevent shattering during the collision process (Ulusay et al., 2007; Aydin, 2009).

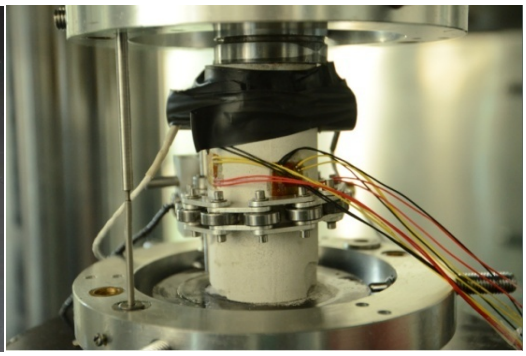

Fig.2 Spherical gypsum samples of different sizes Fig.3 Standard specimen under a uniaxial compression test

In order to explore the effect of different cushion thicknesses and particle sizeson the rolling motion of a rockfall, massive gypsum boards with thesame propertiesas the blocks were

broken,and gypsum particles for simulating the gravel cushion were divided by coarseness using0.2cm, 0.6cm, 1.0cm, 1.4cm, 1.8cmand 2.4cmsieves (Figure 4).

Fig.4 Sieved granules of different particle sizes

A simple rolling stone releasing device is shown in Figure 5, atube with adjustable inclination and height is used to adjust the translational impact velocity of the blocks (Asteriou et al., 2012). The blocks slide and roll through the tube to collide with the plate. Two synchronized digital cameras (1024×1024 pixels and a 200 fps capture rate) were used to acquire the velocities of the blocks in stereoscopic space (Bouguet, 2008; Asteriou et al., 2013).

The two cameras, which obtained the motion, velocity, and kinetic energy automatically, were placed symmetrically at a distance of approximately 0.9m from the impact surface (Figure 5). The distance between the two cameras was about 1.2m, making the cameras look down slightly at the targeted platform.

The synchronized recordings from the two cameras captured a sequence of image stereopairs at time intervals of 1/200 s. By applying stereo-photogrammetric processing, the position of any point in both images can be computed in 3D space. In general, a digital image is a perspective projection of 3D space to the camera lenses. The image plane has a 2D coordinate system where position measurements can be made using pixel coordinates. The camera has a 3D reference coordinate system that is based on the image plane pointing in the viewing direction of the camera. The speed of the rocks can be obtained by measuring the distance they have moved between adjacent frames.

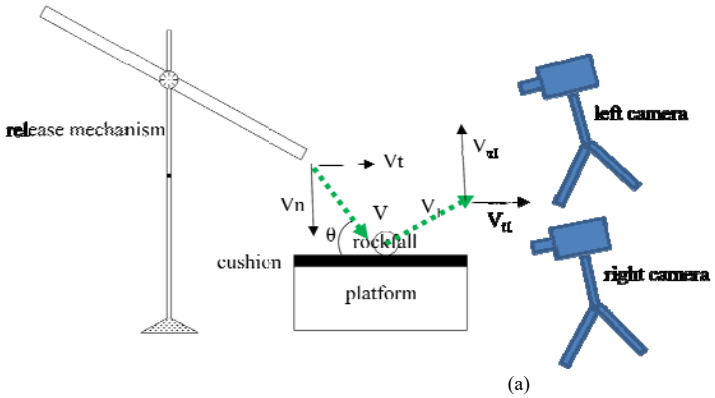

(a)

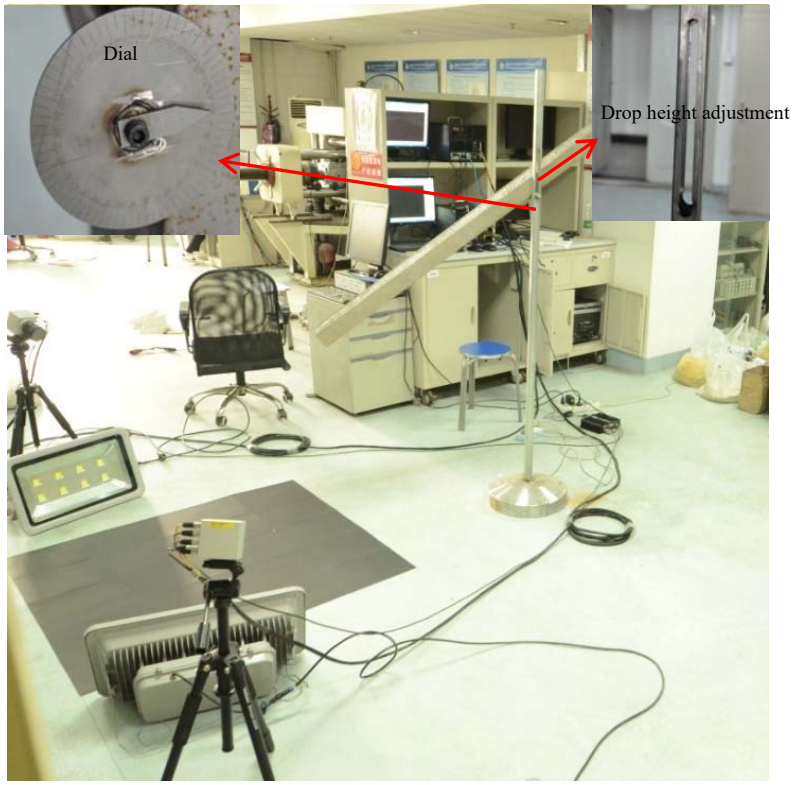

(b)

Fig.5 The experimental apparatus. (a) Model, (b) Laboratory

To simulate gravel cushions of different thicknesses, a large number of 40 cm length × 40 cm width × 2cmheight hollow gypsum boards were made. A 30cm length × 30cm width × 2cm height section was cut out of the center of each board. The hollow gypsum boards were stacked on top of each other to simulate gravel cushions of different thickness, and then the hollow parts of the boards were filled with gypsum particles. The hollow boards were fixed to a massive 40cm length × 40cm width × 6cm height gypsum base to ensure the preservation of momentum from the impact. In order to accurately measure the speed of the blocks with the cameras and to avoid interference from the motion of cushion particles affected by the collision, the cushion was blackened (Figure 6).

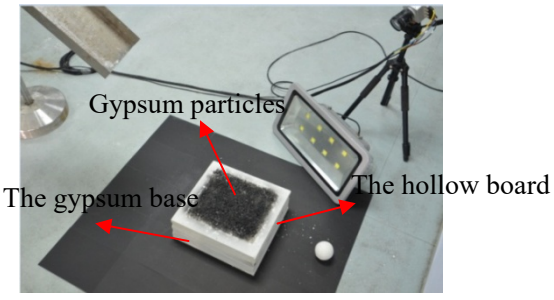

Fig. 6 Laboratory test of rolling blocks

3.2 Experimental procedure

The main uncertainties in the test results arise in tests with large cushion particles, where the wider scatter of the values is attributed to the contact configuration between the large cushion particles and the blocks: large cushion particles have numerous different configurations. This also

affected the deviation in the trajectory caused by the impact, which had a drastically higher uncertainty than for small cushion particles. In order to counteract the effects of chance, a “three tests for the mean” method was adopted, and the average value was set as the final result for each data point in the figures and tables presented here. For cushion particle sizes of 1.8cm and 2.4cm, each test was repeated five times, and the middle three values were used to obtain the average value, while for cushion particle sizes of less than 1.8 cm, each test was conducted three times. If an obviously outlying result was obtained, the test was repeated to reduce the error.

The 2cm, 3cm, 4cm, 5cm radius spherical blocks (Figure 3) were released from a height of 1.2m height, and the effects of cushion thickness and particle size and of block volume on the COR were studied. V_{COR} for the CORs measured in the experiment was calculated using the magnitudes of the incident and rebound velocities as in Equation (1).The block was inserted into one side of the tube and, after sliding and rolling through the tube, collided with the collision surface. The initial impact surface was the massive gypsum base to simulate the platform before paving with a cushion in an open-pit mine. Paved tests were then performed using thicknesses of 2cm, 4cm, 6cm, 8cm, 10cm, 12cm, and 14cm and cushion particle sizesof0.2cm, 0.6cm, 1.0cm, 1.4cm, 1.8cmand 2.4cm. Five iterations of 628 testing cases were carried out.

In order to investigate the effect of rockfall released from different movementheights on the COR of the collision between rockfall and cushion, experiments were conducted in which blocks of 2cm, 3cm, 4cm and 5cmradius fell from 0.4m, 0.8m, 1.2m, and 1.6m to collide with an8-cm thick cushion of different particle sizes. Four iterations of 352 testing cases were carried out. Photographs of the cushion before and after a rock impact experiment are shown in Figure 7.The cushion was always repaired completely after each impact experiment to ensure that the next experiment was free from interference. If any particles had collided out from the platform, new particles were added to supplement the cushion, and the surface was blackened again before the next impact experiment in order for the cameras to obtain accurate measurements of block speed.

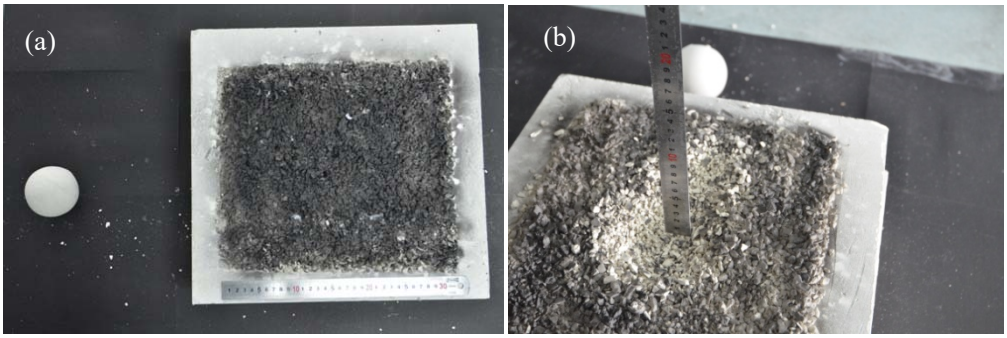

Fig. 7 Photographs of a cushion (a) before and (b) after arock impact experiment

3.3 Experimental results and discussion

3.3.1 Experimental results

The *COR* for blocks released from a height of 1.2m to collide with an uncushioned plate is shown in Figure 8.

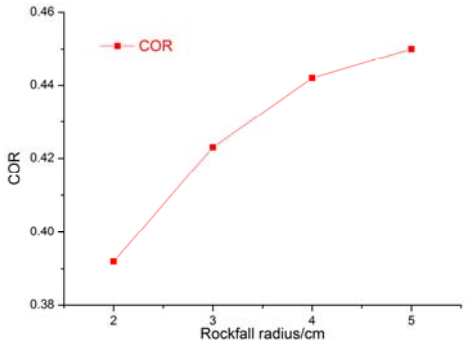

Fig. 8 The COR of block collisions with the plate

CORs derived from experiments where rockfalls of different radii were released from a 1.2m movement height to collide with a paved plate with various cushion thicknesses and particle sizes are plotted in Figure 9.

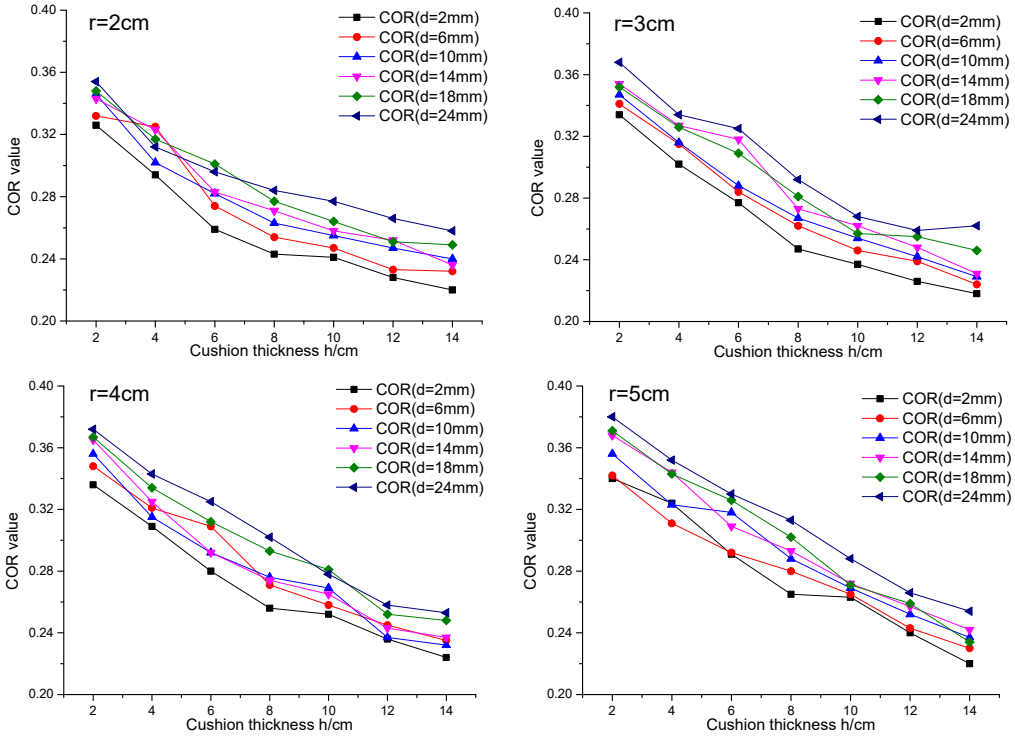

Fig.9 Comparison of the COR of different blocks released from a height of 1.2m

CORs derived for rockfalls of different radii released from different movement heights to collide with an8-cm thick cushion of various particle size are plotted inFigure10.

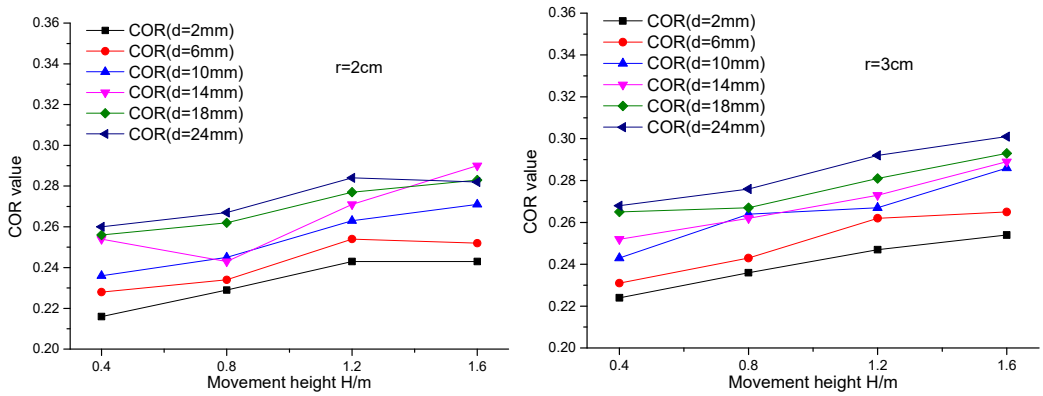

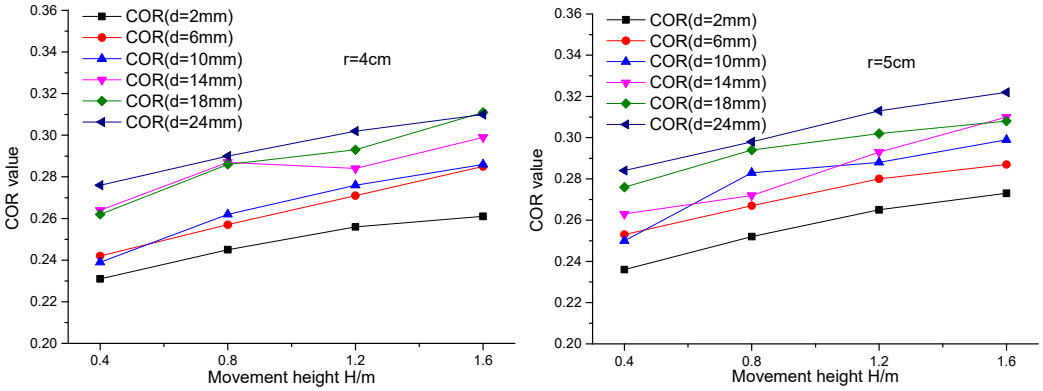

Fig.10 Comparison of the COR for different blocks colliding with an 8-cm thick cushion

3.3.2 Discussion

The figures above indicate that cushion thickness and particle size have a strong influence on the COR of collisions between a rockfall and a cushion, whereas the influence of rockfall block radius is relatively weak. When the particle size of the cushion is small and its thickness is large, the COR of the collision is small, and its effectiveness for energy-consumption is obvious. With an increase in rockfall block radius and movement height, the impact energy increases dramatically for rockfalls colliding with a cushion (Kawahara et al., 1998). Under low impact energy, changes in cushion thickness have a relatively small effect on the COR of the collision between rockfall and cushion, and even thin cushions have a certain energy-absorbing effect, as verified by Pei (2016) and Kawahara (2006). However, under high impact energy, the difference in energy-absorption of different thicknesses of gravel cushion is marked. Because a thin cushion can be more easily compressed in a very short time, the rockfall is more likely to be affected by the underlying platform at low cushion thicknesses. This makes reducing the cushion thickness equivalent to increasing the effective stiffness of the cushion, significantly limiting its buffering and energy-absorbing effect. When the cushion thickness is relatively small, the COR increases significantly with a decrease in cushion thickness. However, when the cushion's thickness is relatively large, this trend is no longer obvious.

When a constant rockfall release height of 1.2m is used, the COR is large where there is no cushion and decreases significantly with an increase in cushion thickness, which agrees with the observations of Kawahara (2005). However, when the cushion reaches a certain thickness, namely, the ratio of the falling block radius,*r*, to the cushion thickness,*h*, is 1/4–1/3, the rate of reduction in the COR with an increasein cushion thickness gradually decreases.COR is more sensitive to the thickness ofcushions with asmall particle size than those witharelatively large particle size:the range inCORscaused bythicknessvariationis wider for small cushion particle sizes, while, as thethickness of cushions with a large particle size is increased, the COR of the collision between rockfall and cushionchangesrelatively slightly.

If the cushion thickness is kept constant at 8cm, as the movement height of the block increases the COR also increases, but when blocks of different radii collide with a cushion of the same thickness, the range in the COR of blocks with a large radius is larger than for blocks with a relatively small radius. When the blocks move from a relatively low height, the COR of the collision between rockfall and cushion is more likely to be affected by the particle size compared to when blocks are released from a greater height. When the cushion particle size is large, the difference in collision configuration between the rockfall and cushion is more pronounced, resulting in a wide range in the COR of the collision between rockfall and cushion.

4Orthogonal test design

4.1 Orthogonal test procedure

To explore the degree of influence of cushion particle size and thickness on *COR* when a rockfall moves through the cushion, orthogonal test theory was adopted to design a test program (Tao et al., 2017). Orthogonal testing is a design method that allows testing of multiple factors and multiple levels. It is based on orthogonality and selects representative points from a comprehensive experiment for testing. The orthogonal test method has the advantages of being uniformly dispersed, neat and comparable, making each test highly representative so that fewer trials can fully reflect the impact of the variation of each factor on the index.

When these factors cannot be considered in full, the leading factor is considered to achieve the expected effects to a great extent. Four parameters, the rockfall block radius,*r*, movement height,*H*, cushion thickness, *h*, and particle size, *d*, were selected as the basic factors to test. The purpose of doing an orthogonal test is to explore the degree of influence of the four different factors on the COR and damage depth, *L*, and find the best combination to reach the optimal protective effect when a rockfall collides with a cushion. The damage depth (*L)* is the depth to which the cushion is influenced after a rockfall has collided with it and can be used to represent the degree of damage to the cushion. As shown in Table 1, every factor has four levels:

Table 1Factors and levels of the orthogonal test

Factor level	Rockfall radius ***r/cm***	Movement height ***H/m***	Cushion thickness ***h/cm***	Particle size ***d/cm***
Level 1	2	0.4	2	0.2
Level 2	3	0.8	4	0.6
Level 3	4	1.2	6	1.0
Level 4	5	1.6	8	1.4

In order to improve the accuracy of the test, and considering that all of the factors have four levels, the L_{32} (4^9) arrangement factor can be selected for the testing program. The damage depth,*L*, of the cushion and the COR of the collision between rockfall and cushion are taken as test indices to explore the degree of influence of the four factors (Pichler et al., 2005).

As there is a high degree of randomness inherent in the rockfall motion, each case was tested three times and the mean value was taken as the final result, so as to improve the accuracy of the experiments. The test results are shown in Table2.

Table 2 Orthogonal test results

Test number	Rockfall radius***r/cm***	Movement height ***H/m***	Cushion thickness***h/cm***	Particle size ***d/cm***	Damage depth of cushion ***L/cm***	***COR*** of collision between rockfall and cushion
1	2	0.4	2	0.2	0.65	0.278
2	2	0.8	4	0.6	0.74	0.273
3	2	1.2	6	1.0	0.93	0.282

4	2	1.6	8	1.4	1.05	0.295
5	3	0.4	2	0.6	0.58	0.294
6	3	0.8	4	0.2	1.45	0.265
7	3	1.2	6	1.4	1.03	0.317
8	3	1.6	8	1.0	1.60	0.280
9	4	0.4	4	1.0	0.62	0.296
10	4	0.8	2	1.4	0.56	0.338
11	4	1.2	8	0.2	2.60	0.256
12	4	1.6	6	0.6	2.20	0.284
13	5	0.4	4	1.4	0.61	0.309
14	5	0.8	2	1.0	0.58	0.328
15	5	1.2	8	0.6	2.12	0.280
16	5	1.6	6	0.2	2.85	0.273
17	2	0.4	8	0.2	1.36	0.216
18	2	0.8	6	0.6	1.24	0.265
19	2	1.2	4	1.0	1.13	0.302
20	2	1.6	2	1.4	0.68	0.358
21	3	0.4	8	0.6	0.92	0.231
22	3	0.8	6	0.2	1.49	0.256
23	3	1.2	4	1.4	1.08	0.327
24	3	1.6	2	1.0	0.84	0.351
25	4	0.4	6	1.0	0.77	0.287
26	4	0.8	8	1.4	0.81	0.281
27	4	1.2	2	0.2	1.03	0.336
28	4	1.6	4	0.6	1.96	0.318
29	5	0.4	6	1.4	0.67	0.292
30	5	0.8	8	1.0	1.05	0.275
31	5	1.2	2	0.6	1.14	0.347
32	5	1.6	4	0.2	2.54	0.294

4.2 Optimization analysis and discussion of test results

4.2.1 Optimization analysis method (flow)

The analysis method used to optimize the calculation results and the optimization process is shown in Figure 11.

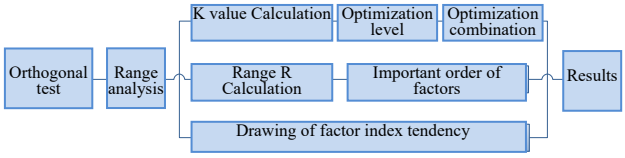

Fig.11Flowchart for the optimization analysis ofthetest

The four parameters, rockfall block radius,$\boldsymbol{r}$, movement height,H, cushion thickness, h, and particle size, d, belong to the factor set $x \in$(A, B, C, D), and the number of levels for all factors is four. The statistical test parameter under level $\boldsymbol{y}$ of factor set X can be calculated by determining K_{xy} (x=A, B, C, D; y=1, 2, 3, 4), i.e., the sum of all the test result indices P_{xy} containing level Y of factor X, and dividing it by the total number of levels to obtain the average value k_{xy} in which P_{XY}

is the random variable of the normal distribution:

$$k_{\mathrm{xy}} = \frac{K_{\mathrm{xy}}}{4} = \sum P_{xy} \Big/ 4 \quad , (6)$$

where K_{xy} is the statistical parameter of factor $\boldsymbol{x}$ at level $\boldsymbol{y}$, k_{xy} is the average value of K_{xy}, and R_y is the range of factor$\boldsymbol{y}$.

k_{xy} can be used to judge the optimization level and optimization combination of each factor. If a more optimal result is obtained at a higher index value, then the level that increases the index value should be selected, i.e., the level with maximum values for all factors k_{xy}; conversely, if the smaller the index value is, the more optimalit is, the level with minimum values for all factors k_{xy} should be selected. The parameter combination corresponding to an optimal level of all factors is the optimal parameter combination. R_y reflects the amount of variation of the test index when factor level y is fluctuating. The larger R_y is, the more sensitive the factor is to the influence of the test index. The order of importance of the factors can be judged using R_y, and the optimization level and optimization combination of factor x can be judged from k_{xy}.

4.2.2 Results of analysis and discussion

Range analysis was used to analyze the orthogonal test results in Table 2. If the influencing factors for the range analysis are the damage depth,*L,* of the cushion and the COR of the collision between rockfall and cushion (Table 3), then the optimum parameter combination for rockfall block radius,*r*, movement height,*H*, cushion thickness, *h*, and particle size, *d*, to reduce COR can be obtained.

Table 3 Influencing factor range analysis of all evaluation indices

Evaluation index	Levels	Rockfall radius ***r/cm***	Movement height ***H/m***	Cushions thickness ***h/cm***	Particle size ***d/cm***
COR of collision between rockfall and cushion	k_1	0.285	0.271	0.325	0.270
	k_2	0.288	0.287	0.296	0.285
	k_3	0.298	0.305	0.281	0.301
	k_4	0.299	0.306	0.267	0.313
	R_y	0.014	0.035	0.058	0.043
Damage depth of cushion ***L***	k_1	0.97	0.78	0.76	1.75
	k_2	1.12	0.99	1.26	1.35
	k_3	1.33	1.38	1.40	0.94
	k_4	1.44	1.72	1.44	0.81
	R_y	0.47	0.94	0.68	0.94

The following conclusions can be derived from Table 3:

(1) The degree of influence of the factors considered on the COR of the collision between rockfall and cushion is: cushion thickness (*h*)>particle size (*d*)>movement height *(H)*>block radius (*r*);

(2) The degree of influence of the factors considered on the damage depth,*L*, of the cushionis: particle size (*d*)=movement height (*H*)>cushion thickness (*h*)>block radius (*r*).

E-I tendency figures (Tao et al., 2017) are used to further explore the effects of each factor on the test indices. The level of all factors is the X-coordinate (*E*), and the average value of the test index is the Y-coordinate (*I*). The *E-I* tendency drawings shown in Figure 12 and Figure 13 intuitively reflect the tendency of the test index with a change in factor level and can point the way

to further testing.

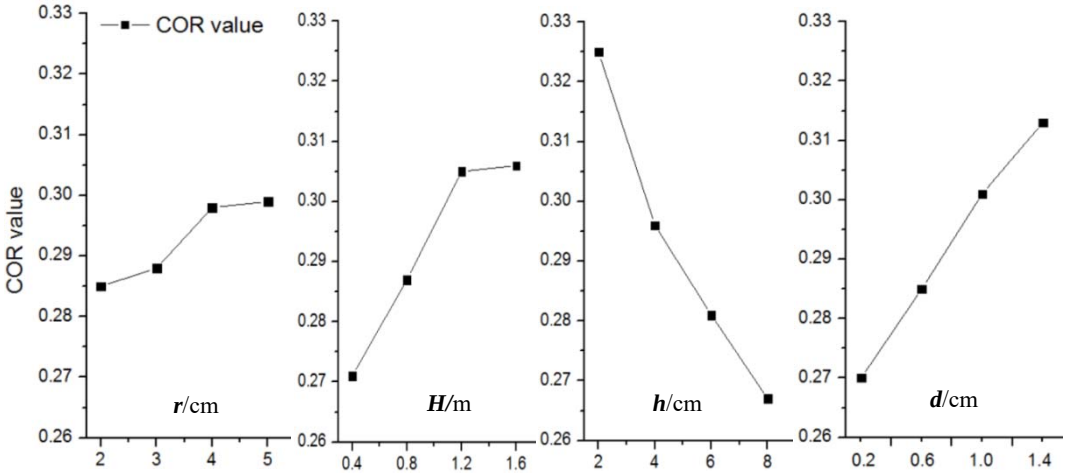

Fig.12 Tendency of each factor as regards the COR of the collision between rockfall and cushion

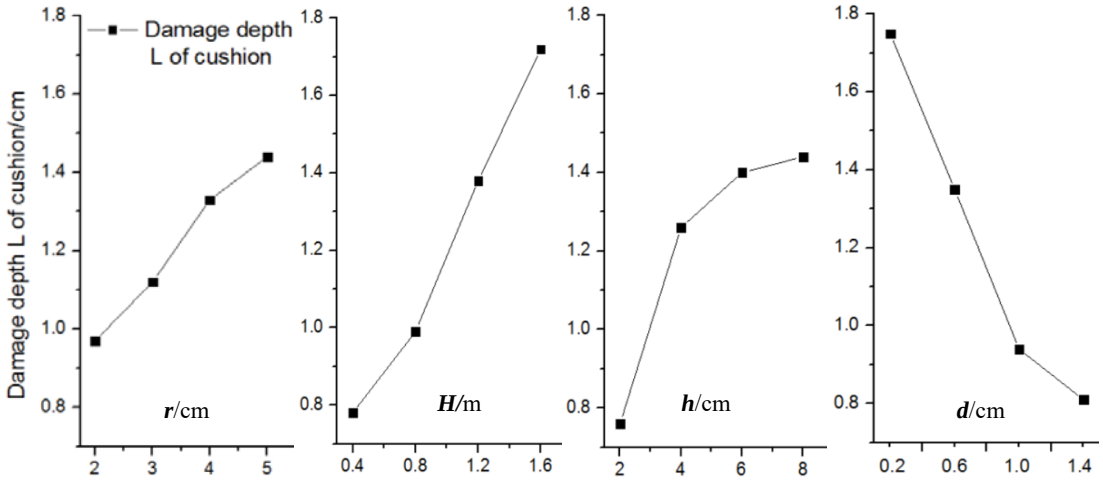

Fig.13Tendency of each factor as regards damage depth ***L*** of the cushion

The following conclusions can be derived from Figures11and12:

(1) The smallest optimal parameter combination of the COR of the collision between rockfall and cushion is A1B1C4D1; that is, when *r*=2cm, *H*=0.4m, *h*=8, *d*=1.4, the *COR* of the collision between rockfall and cushion is the smallest (Figure 12).

(2)The shallowest optimal parameter combination of damage depth,*L,*of the cushion isA1B1C1D4; that is, when *r*=2cm, *H*=0.4m, *h*=2, *d*=1.4, the damage depth,*L*, of the cushion is the shallowest (Figure 13).

To sum up, the cushion thickness,*h*, has the most significant influence on the COR of the collision between rockfall and cushion, while it has arelatively minor effect on the damage depth,*L*, of the cushion. The second most importantfactoris particle size,*d*, but the cushion can easily be destroyed when arockfall with a high kinetic energy collides with a cushion of small particle size. The degree of influence of the rockfall block radius,*r*, on the two indicesis far less than that of the other factors. When a gravel cushion is used to control rockfall down a slope, the effectiveness with which it controls the rockfall and its durability is taken into account (Pichler et al., 2005) so the cushion thickness,*h*, should be the primary consideration in cushion design. The optimal thickness is 3–4 times the radius of the majority of the rockfall blocks. The smaller the particle size is, the smaller the COR is, but the cushion is also more likely to be destroyed so the

appropriate particle size must be determined by combining the expected and evaluated block size and drop height of the rockfall so that the cushion not only achieves the effect of reducing COR but also maintains its stability.

5 Conclusions

The buffering and energy-dissipation mechanism of gravel cushions with different properties under different impact energies were studied through laboratory collision tests, leading to in the following conclusions:

1. Unlike conventional protection measures, a gravel cushion makes full use of waste mullock produced in the process of mine extension, which can be conveniently broken up into particles of the appropriate size. This can not only reduce the costs of reducing rockfall hazard and of mullock transportation and relieve overloading of the mine's dump but can also achieve better control of rockfalls, realizing the goal of "stone conquers stone."

2. Through laboratory tests of cushions with different parameters, varying both the radius (and hence mass) of the falling block and its drop height, it is found that a change in the thickness of the cushion has a more significant effect on the COR of the collision between rockfall and cushion under the impact of a rockfall with high impact energy than under the impact of a rockfall with low impact energy. When the cushion reaches a certain thickness, namely, the ratio of the falling block radius,r, to the cushion thickness,h, is 1/4–1/3, the rate of reduction in the COR with an increase in cushion thickness gradually decreases. When the blocks move from a relatively low height, the COR of the collision between rockfall and cushion is more likely to be affected by the particle size compared to when blocks are released from a greater height. Therefore, in the process of cushion design, the estimated physical properties and drop height of the potentially dangerous rock should be investigated to roughly estimate the impact energy of the rockfall.

3. Through an orthogonal test, it is found that the cushion thickness,h, has the most significant influence on the COR of the collision between rockfall and cushion. The second most importantfactor is particle size,d, but the cushion can easily be destroyed when a rockfall with a high kinetic energy collides with a cushion of small particle size.Therefore, the optimum cushion thickness and particle size can be obtained by taking its effectiveness, its structural reliability, and any economic constraints into account. The smaller the particle size is, the smaller the COR is, but a cushion with a small particle size is more likely to be destroyed. The appropriate particle size must be determined on the basis of the block size and drop height of the expected rockfall so that the cushion can not only achieve the effect of reducing COR but also maintain its stability.

4. Until now, it has not been possible to dictate a universal rule that the majority of engineering personnel can follow in the design of gravel cushions for a platform. This is a troubling blind spot. However, this work shows that, as well as increasing the cushion thickness, changing its particle size can improve the rockfall-controlling effect, and that the optimal particle size can be determined on the basis of the expected block size and drop height of the rockfall. This provides a widely applicable theoretical and practical basis for cushion design for open-pit mine rockfall protection.

References

[1] Huang, R. Q., Liu, W. H., Zhou, J. P., and Pei, X. J. Rolling tests on movement characteristics of rock blocks. Chinese Journal of Geotechnical Engineering, 2007, 29(9):1296-1302. (in Chinese)

[2] Pantelidis, L. Rock slope stability assessment through rock mass classification systems. International Journal of Rock Mechanics and Mining Sciences, 2009, 46(2): 315-325.

[3] Pantelidis, L. An alternative rock mass classification system for rock slopes. Bulletin of engineering geology and the environment, 2010, 69(1):29-39.

[4] Heidenreich B. Small- and half-scale experimental studies of rockfall impacts on sandy slopes. Dissertation, EPFL, 2004.

[5] V Labiouse, B Heidenreich Heidenreich. Half-scale experimental study of rockfall impacts on sandy slopes. Natural Hazards & Earth System Sciences,2009, 9(6):1981-1993.

[6] EP Howald, JM Abbruzzese, C Grisanti. An approach for evaluating the role of protection measures in rockfall hazard zoning based on the Swiss experience. Natural Hazards & Earth System Sciences, 2017, 17(7):1127-1144.

[7] C Mignelli, D Peila, SL Russo, et al. Analysis of rockfall risk on mountainside roads: evaluation of the effect of protection devices. Natural Hazards, 2014, 73(1):23-35.

[8] Thornton C, Ning Z. A theoretical model for the stick/bounce behavior of adhesive, elastic–lastic spheres. Poeder Technology, 1998, 99 (2):154-162.

[9] Pavlos Asteriou, George Tsiambaos. Empirical Model for Predicting Rockfall Trajectory Direction. Rock Mech Rock Eng, 2016, 49:927-941.

[10] Topal T, Akın M, Özden AU. Analysis and evaluation of rockfall hazard around Afyon Castle, Turkey. Environmental Geology, 2006, 53 (1) :191-200.

[11] Koleini M, Van Rooy JL Falling rock hazard index: a case study from the Marun Dam and power plant, south-western Iran. Bull Eng Geol Environ,2011, 70 (2) :279-290.

[12] Saroglou H, Marinos V, Marinos P, Tsiambaos G. Rockfall hazard and risk assessment: an example from a high promontory at the historical site of Monemvasia, Greece. Nat Hazards Earth Syst Sci, 2012, 12(6):1823–1836.

[13] Sadagah B. Back analysis of a rockfall event and remedial measures along part of a Mountainous Road, Western Saudi Arabia. Int J Innov Sci Mod Eng (IJISME). 2015,3(2): 2319-6386.

[14] RI Leine, A Schweizer, M Christen, et al. Simulation of rockfall trajectories with consideration of rock shape. Multibody System Dynamics, 2014,32(2):241-271.

[15] Huang, R. Q., Liu, W. H., Gong, M. F., and Zhou, J. P. Study of trees resistance effect test on rolling rock blocks. Chinese Journalof Rock Mechanics and Engineering, 2010, 29(s1):2895-2901. (in Chinese)

[16] S. Notaro, A. Paletto. The economic valuation of natural hazards in mountain forests: an approach based on the replacement cost method. J. For. Econ, 2012, 18 (4): 318–328.

[17] JM Monnet， F Bourrier， S Dupire, et al. Suitability of airborne laser scanning for the assessment of forest protection effect against rockfall. Landslides, 2017,14(1):299-310.

[18] SD Miranda, C Gentilini, G Gottardi, et al. Virtual testing of existing semi-rigid rockfall protection barriers. Engineering Structures, 2015, 85:83-94.

[19] Kishi N，Bhatti A Q． An equivalent fracture energy concept for nonlinear dynamic response analysis of prototype RC girders subjected to falling-weight impact loading. International Journal of Impact Engineering，2010, 37(1):103－113．

[20] Kishi N，Konno H，Ikeda K，et al． Prototype impact tests on ultimate impact resistance of PC rock-sheds. International Journal of Impact Engineering, 2002, 27(9):969－986．

[21] Bhatti A Q，Kishi N． Impact response of RC rock-shed girder with sand cushion under falling load. Nuclear Engineering and Design, 2010, 240(10):2626-2632．
[22] Bhatti A Q，Kishi N，Mikami H，et al． Elasto-plastic impact response analysis of shear-failure-type RC beams with shear rebars． Materials ＆ Design, 2009, 30(3):502－510．
[23] Badger, T. C., Duffy, J. D., and Schellenberg, K., “Chapter 14-Protection,” Rockfall Characterization and Control.2009:48-62.
[24] F. Delhomme, M. Mommessin, J. P. Mougin, and P. Perrotin. Behavior of a structurally dissipating rock-shed: experimental analysis and study of punching effects. International Journal of Solids and Structures, 2005, 42(14):4204–4219.
[25] M. Mommessin, A. Agbossou, F. Delhomme et al. Horizontal and slanting reinforced concrete slabs for structurally dissipating rock-shed: experimental analysis. In Proceedings of the 5th International Conference on Fracture Mechanics of Concrete and Concrete Structures, V. C. Li, C. K. Y. Leung, and K. J. Willam, Eds., 2004, 2(1):965–972, American Concrete Institute, Vail, Colo, USA.
[26] S. Kawahara, T. Muro. Effects of dry density and thickness of sandy soil on impact response due to rockfall. Journal of Terramechanics, 2006, 43 (3): 329–340.
[27] S Lambert, A Heymann, P Gotteland, et al. Real-scale investigation of the kinematic response of a rockfall protection embankment. Natural Hazards & Earth System Sciences, 2014,14(5):1269-1281.
[28] J Sun, Z Chu, Y Liu, et al. Performance of Used Tire Cushion Layer under Rockfall Impact. Shock and Vibration, 2016, 2016 (10):1-10.
[29] Heierli W, Merk A, Temperli A. Schutz gegen Steinschlag—Protection contre les chutes de pierres [Protectionagainst rockfall]. Forschungsarbeit 6/80. Vereinigung Schweizerischer Strassenfachleute (VSS), 1981 [in German].
[30] Labiouse V, Descoeudres F, Montani S. Experimental study of rock sheds impacted by rock blocks. Struct Eng Int, 1996, 6(3):171–176.
[31] Giani GP (1992) Rock slope stability analysis. Balkema, Rotterdam.
[32] Chau KT, Wong RHC, Wu JJ. Coefficient of restitution and rotational motions of rockfall impacts. Int J Rock Mech Min Sci 2002, 39(1):69–77.
[33] Yang Youkui, Zhou Yingqing, Jiang Ruiqi, et al. Theory and practice of slope geological disaster flexible protection [M].Beijing: Science Press, 2005. (in Chinese)
[34] Zhu C., Tao Z., Yang S., Zhao S. V shaped gully method for controlling rockfall on high-steep slopes in China. Bulletin of Engineering Geology and the Environment, 2018 (In Press). DOI: 10.1007/s10064-018-1269-7.
[35] Ulusay R, Hudson JA. The complete ISRM suggested methods for rock characterization, testing and monitoring: 1974–2006. Ankara: ISRM Commission on Testing Methods; 2007.
[36] Aydin A. ISRM Suggested method for determination of the Schmidt hammer rebound hardness: revised version. Int J Rock Mech Min Sci. 2009;46(3):627–34.
[37] Asteriou, P., Saroglou, H., and Tsiambaos, G. “Geotechnical and kinematic parameters affecting the coefficients of restitution for rockfall analysis.” International Journal of Rock Mechanics and MiningSciences, 2012, 54(1):103-113.
[38] Bouguet JY.Camera calibration toolbox for Matlab. http://www.vision.caltech.edu/bouguetj/calib_doc.Accessed 20 Jan,2012.
[39] Asteriou P, Saroglou H, Tsiambaos G Rockfall: scalingfactors for the coefficient of restitution. In: Kwasniewski M,Lydzba D (eds) Rock mechanics for resources, energy and environment. Taylor & Francis Group, London, 2013:195–200.

573 [40] Kawahara S, Muro T. Effects of weight mass and drop height on vertical distribution of dry density of sandy
574 soil in one-dimensional impact compaction. In: Proceedings of the 5th Asia-Pacific regional conference of
575 the ISTVS; 1998:151–61.
576 [41] Pei, X. J., Liu, Y., Wang, D., P. Study on the Energy Dissipation of Sandy Soil Cushions on the Rock-shed
577 Under Rockfall Impact Load. Journal of Sichuan University (Engineering Science Edition), 2016,
578 48(1):15-22.(in Chinese)
579 [42] Pichler B，Hellmich C，Mang H A． Impact of rocks onto gravel design and evaluation of experiments.
580 International Journal of Impact Engineering, 2005, 31(5):559－578.
581 [43] Tao, Z. G., Zhu, C. Test of V shaped groove structure against rockfall based on orthogonal design. Journal of
582 China Coal Society, 2017, 42(9):2307-2315.